

Mixed Hardware and Software Embedded Signal Processing Methods for *in-situ* Analysis of Cardiac Activity

Bertrand Massot¹, Tanguy Risset², Gregory Michelet¹ and Eric McAdams¹

¹Lyon Institute of Nanotechnology, CNRS - INSA Lyon, University of Lyon, Villeurbanne, France

²Centre of Innovation in Telecommunications and Integration of Service, INRIA - INSA Lyon, Villeurbanne, France

Keywords: Wearable Sensors, Heart Rate, Heart Rate Variability, Biomedical Signal Processing, Body Sensors Network.

Abstract: This paper presents the implementation of a combination of hardware and software signal processing methods on a wearable device for the continuous and long-term monitoring and analysis of cardiac activity during *in-situ* experiments. Heart rate assessment and heart rate variability parameters are computed in real-time directly on the sensor, thus only few parameters are sent via wireless communication for power saving. Hardware method for heart rate measurement, and software methods for the calculation of time-domain and frequency-domain parameters of heart rate variability are described, and preliminary tests for the evaluation of the sensor are presented.

1 INTRODUCTION

The continuous and long-term monitoring of an individual's vital signs enables a real-time and more relevant health diagnosis, in order to set up appropriate preventive measures, and to undertake rapid remedial action in the case of early detection of symptoms; as, for example, the latent anticipation of sudden cardiac arrest (424 000 annual out-of-hospital cardiac arrests, with an overall survival rate of only 5.2 % (Go et al., 2014)) by evaluating the risks of cardiovascular disease and by detecting any cardiac abnormalities. This in turn will result in more effective healthcare delivery, both financially and therapeutically (Van Hoof and Penders, 2013) by avoiding untimely hospitalization while ensuring patient safety and autonomy.

A promising solution is the development of wearable systems which assess relevant indicators enabling a direct, on-body cardiac diagnosis. Several research projects' results in this area have highlighted a range of various technical challenges that must be overcome (McAdams et al., 2011), (Massot et al., 2013). The achievement of a suitable device for continuous, long-term monitoring of heart rate activity will enable the detection of cardiac abnormalities in the electrocardiogram signal (ECG), for example to prevent ventricular fibrillation (VF), and to monitor the instantaneous heart rate (HR), from which can be derived several parameters regarding heart rate variability (HRV). HRV provides information on autonomic nervous system (ANS) activity, a relevant indi-

cator for several pathologies (Malik et al., 1996) and more generally on an individual's stress and arousal.

New wearable devices for the monitoring of heart rate activity can exploit the benefits of recent technological advances in electronics and wireless communication systems in order to overcome the challenges previously cited. Prototypes developed in laboratories already show really promising results in terms of wearability, robustness and autonomy, as for example the wearable patch developed at the Holst Centre which benefits from both elaborated hardware (Altini et al., 2011) and software (Romero et al., 2009), and more recently from a new kind of dry electrode for comfortable measurements (Chen et al., 2013). There are already commercially available products for personal monitoring of one's own cardiac rhythm, but they are mainly aimed at well-being and fitness applications rather than being suitable for medical prevention and diagnosis. Most of these systems suffers from a lack of accuracy, depending on the sensing method used : for example, plethysmography appears to be still questionable for instantaneous HR and short-term HRV assessment and is highly sensitive to motion artefacts in ambulatory conditions (Schäfer and Vagedes, 2013). Also, filtering and interpolating HR due to motion artefacts induces distortion in frequency content of subsequent HRV parameters.

In this paper, we presents an optimized combination of robust and accurate methods for on-board

HR detection and HRV calculation. The methods were implemented on a programmable system-on-chip which provides hardware analog and digital programmable functions as well as a 32-bit ARM Cortex M3 micro-controller unit. The objective was to optimize the selected methods in order to benefit from the ultra-low power consumption of the hardware part, which is used for real-time HR detection and period measurement, and to reduce the calculation time of frequency-domain parameters of HRV, which is done together with time-domain parameters by the micro-controller unit.

In section 2, the different methods for ECG measurement, HR detection and HRV calculation, as well as their implementation on the targeted device are described. Then the evaluation of the accuracy of the methods, both on test-bench and in real-life conditions is presented in section 3.

2 MATERIALS AND METHODS

2.1 Targeted Wearable Device Overview

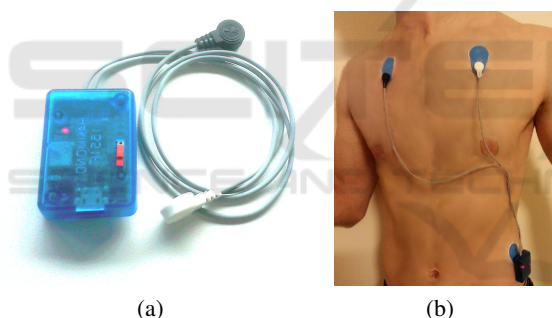


Figure 1: Device overview (a) and example of placement on the body using three disposable electrodes (b).

The REC Heart Activity sensor is a wearable device which has been developed to enable the continuous monitoring and analysis of cardiac activity during long-term experiments in real life conditions.

The device comprises a small electronic board and a 300 mAh Lithium-Ion battery encapsulated in a small plastic enclosure (50 mm x 35 mm x 15 mm) and can be connected to ECG electrodes by the means of three snap connectors, thus the sensor is intended to be connected to various electrode configurations, directly on the body (Figure 1). Possible electrode configurations include for example a disposable patch of gel electrodes, or a chest belt with dry electrodes, depending on the requirements regarding the experiment conditions (resting or effort during short periods, long-term monitoring during several days, etc.). The electronic board includes a Bluetooth Low

Energy (BLE) interface for wireless communication, and the sensor can be integrated in a Wireless Body Sensor Network (WBSN). In the frame of the RE-CAMED project, an Android application has been developed to collect data from a WBSN composed of various wearable sensors including the REC Heart Activity sensor.

The electronic architecture of the board is based on a PSoC 5LP (Cypress Semiconductors). This mixed-signal Programmable System-on-Chip consists of a Cortex M3 ARM micro-controller unit, but also includes analog programmable functions as well as programmable logic device (PLD) based functions. This component can thus carry out all the steps from the conditioning of the ECG signals to the transmission of high level heart activity indicators through the BLE interface, including signal processing, analog to digital conversion, heart beat detection, heart rate measurement, and heart rate variability calculation. All these functions are integrated within a low-power, single chip with a highly reduced size (8 mm x 8 mm) as described in the next sections.

2.2 Integrated Signal Processing of Electrocardiogram

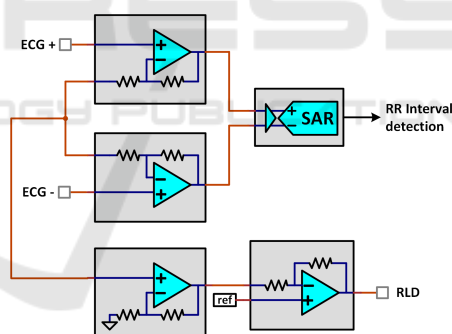


Figure 2: ECG processing chain using internal PSoC 5LP analog hardware components.

The amplification and digitization of ECG is done by using the integrated and programmable analog functions of the PSoC5 LP. A differential amplifier is realized by combining programmable gain amplifiers and the outputs are directly connected to a 12-bit successive approximation differential ADC (Figure 2). Two additional operational amplifiers used as buffer and inverting amplifier respectively are chained to implement a right-leg drive (RLD) circuit to provide additional common-mode noise rejection (Winter and Webster, 1983). The overall differential gain is set to 24 and the SAR ADC has an input range set to ± 1.024 V so the resolution is $20.8 \mu\text{V}/\text{bit}$, and the signal is sampled at 8192 samples per second.

2.3 Integrated Hardware Digital Measurement of Heart Rate

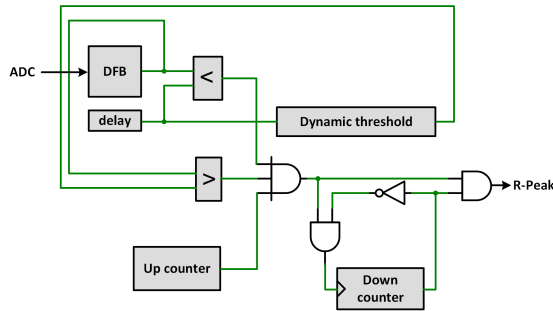


Figure 3: RR-Interval detection chain using internal PSoC 5LP digital hardware components (PLDs).

The objective of using hardware digital components for the measurement of Heart Rate is to benefit for the highly reduced consumption of PLDs available within the PSoC. Consuming processing time of the MCU for R-peak detection would lead to a high usage of battery power for a real-time detection peaks on the ECG signal at a 8192 sps sampling rate. Alternatively this hardware chain have an average consumption of 140 μA and enables the MCU to remains into an idle state, as the data is also directly transmitted from the analog chain to the digital chain by a DMA channel. R-peaks detection is done by implementing a digital filter and a local maximum detector in the PSoC's PLDs (Figure 3).

The digital filter block (DFB) acts as an ultra-low power DSP in which is implemented a non-linear filter to enhance power in the higher frequency of ECG signal (Pan and Tompkins, 1985). The processing includes a double buffering of the ECG to calculate a smoothed derivative which is then squared, and a moving-average filter is applied on the final signal.

The local maximum detector uses an adaptive threshold to take into account the variability of ECG amplitude between individuals and also aver time. The dynamic threshold T is dynamically computed within the PLD components by an exponential filter as in Equation 1, where β is the amplitude ratio of the current peak detected P , and α is the smoothing factor of the filter.

$$T_{n+1} = \alpha \cdot \beta \cdot P_n + (1 - \alpha) \cdot T_n \quad (1)$$

The value of a 1024 Hz up-counter is copied into the MCU memory by a DMA channel and an interrupt is triggered each time a peak is detected on the signal. Additionally a "fail-safe" down-counter disables detection when false peaks have been detected until three consecutive peaks are properly detected. The condition of false detection is true when the variation

of RR-interval is higher than 25% of the last one. This method guarantees reliable RR-intervals value for the proper calculation of HRV parameters which is more sensitive to false detection than missing values (cf. section 2.4).

2.4 Software Calculation of Heart Rate Variability Parameters

When the hardware detector triggers an interrupt which wakes up the MCU, the new RR-interval is copied into a buffer which keep in memory the values of the last 5 minutes, the standard period for evaluating short-term HRV according to the Task Force of the European Society of Cardiology and the North American Society of Pacing and Electrophysiology (Malik et al., 1996). This signal (tachogram) buffered is then used to calculate both time-domain and frequency-domain parameters of HRV. The Task Force has selected a large number of parameters to evaluate HRV, from which four parameters has been retained to be calculated in this application, based on their common usage in the analysis of ANS activity (see Table 2 at the end of the section).

The calculations are performed directly by the MCU with floating point values, due to the precision needed within these operations. This induces periods of intensive occupation of the MCU which need to be reduced at the minimum if one wants to optimize consumption of the device.

2.4.1 Time-domain Parameters

The calculation of time-domain parameters of the HRV is quite straight-forward and the two most used parameters are computed in this application, i.e. the standard deviation of intervals in the buffer (SDNN) and the quadratic mean of differences between successive intervals (RMSSD). These parameters are calculated used the formulas given by Equations 2 and 3.

$$\text{SDNN} = \sqrt{\frac{1}{n-1} \left(\sum_{i=1}^n (\text{RR}_i)^2 - \frac{1}{n} \left(\sum_{i=1}^n \text{RR}_i \right)^2 \right)} \quad (2)$$

$$\text{RMSSD} = \sqrt{\frac{1}{n-1} \left(\sum_{i=1}^{n-1} (\text{RR}_{i+1} - \text{RR}_i)^2 \right)} \quad (3)$$

Most devices commercially available which provide real-time HRV monitoring, calculate only one time-domain parameter (one among the two cited), and usually without naming it. In this application, we

apply to provide precise information about the parameters calculated, whose variations can differ depending on the situation and thus modify the interpretation of HRV regarding the ANS activity.

2.4.2 Frequency-domain Parameters

Calculation of frequency-domain parameters of HRV requires an evaluation of power spectral density (PSD) of the tachogram as it evaluates the distribution of energy of the signal in separated frequency bands. The main frequency bands are usually defined as ultra-low (ULF), very low (VLF), low (LF) and high frequencies (HF) (Table 1).

Table 1: Separation of power spectral density of the tachogram in frequency bands.

Name	Frequency range
ULF	≤ 0.003 Hz
VLF	0.003-0.04 Hz
LF	0.04-0.15 Hz
HF	0.15-0.4 Hz

In this application, the method of evaluating the PSD is critical due to the embedded electronic architecture used in the sensor, which provides limited resources in performance and time. As RR-intervals vary in time, the tachogram is composed of unevenly sampled values; thus a traditional approach for spectral analysis consists of a combination of (i) an interpolation, in order to recover an evenly sampled signal, and (ii) a subsequent Fast Fourier Transform (FFT) to obtain the PSD. However this approach, depending on the method of interpolation, the sampling rate and the number of points, is known to introduce distortion in the high-frequency domain where re-sampling acts as a low-pass filter, leading to an overestimation of HRV parameters (Clifford and Tarassenko, 2005). Also this method is known to be very sensitive to both errors in detection and measurement of RR-intervals as well as missing values in the tachogram.

Another approach for spectral analysis of an unevenly sampled signal is the least square analysis, commonly termed the Lomb-Scargle periodogram, which provides (in a normalised form), the estimated power P of the angular frequency component ω . The estimated power is given by Equation 4, where $\sigma =$ SDNN, the standard deviation of all R-R intervals, \overline{RR} is the mean value, and τ is an angular quantity defined by Equation 5.

$$P(\omega) = \frac{1}{2\sigma^2} \left(\frac{[\sum_{i=1}^n (RR_i - \overline{RR}) \cos(\omega(t_i - \tau))]^2}{\sum_{i=1}^n \cos^2(\omega(t_i - \tau))} + \frac{[\sum_{i=1}^n (RR_i - \overline{RR}) \sin(\omega(t_i - \tau))]^2}{\sum_{i=1}^n \sin^2(\omega(t_i - \tau))} \right) \quad (4)$$

$$\tan(2\omega\tau) = \frac{\sum_{i=1}^n \cos(2\omega t_i)}{\sum_{i=1}^n \sin(2\omega t_i)} \quad (5)$$

This method, originally proposed by Lomb (Lomb, 1976) and further elaborated by Scargle (Scargle, 1982), was proposed as a surrogate for HRV calculations for the first time by Shin et al. (Shin et al., 1994) in 1994 (to the best of authors' knowledge). This method provides better accuracy and lower noise levels in the estimation of the density power spectrum, but unfortunately it also has the major drawback of involving much more calculation complexity, and thus MCU time consumption, even when the algorithm is optimized with classical trigonometric recurrences.

Press and Rybicki (Press and Rybicki, 1989) have proposed a much faster computation of this parameter by combining the accuracy of the periodogram and the efficiency of FFT, resulting in an algorithm which is as fast as two FFT calculations and a $N \log N$ order instead of N^2 . In this case the FFT is not used for the direct evaluation of the periodogram, but rather to calculate approximately (but to any desired precision), both main terms of Equation 4. To evaluate trigonometric sums of the equation, which can not be calculated with FFTs due to the unevenly spaced data, the method involves reverse interpolations, call extirpolation. As the interpolation evaluates one value at an arbitrary point upon several values from a regularly sampled function, the extirpolation evaluates several value of a regularly sampled function from the value of an arbitrary point. The precision, and also the duration of this evaluation depends on the number of extirpolated points per 1/4 cycle of the highest frequency (MACC parameter). The raw algorithm and several values of the MACC parameter of its fast implementation have been tested, and a performance comparison in accuracy and gain of time is presented in the Results section.

As stated above, the Lomb-Scargle periodogram being dedicated to the evaluation of PSD for unevenly signals, it is far less sensitive to missing data than FFT where interpolation can lead to large differences depending on the interpolation method. Also both methods are sensitive to false detections, therefore an additional "fail-safe" digital circuit has been added to the R-peak detector as described in section 2.3. This circuit gives a higher prevalence to correct R-peak detections at the cost of additional missing values.

Table 2: Summary of short-term HRV parameters calculated by the REC Heart Activity sensor.

Variable	Unit	Domain	Description
SDNN	ms	Time	Standard deviation of all R-R intervals
RMSSD	ms	Time	Quadratic mean of differences between successive R-R intervals
LF/HF	n.u.	Frequency	Ratio between LF and HF components of the PSD of all R-R intervals
LF norm	%	Frequency	Ratio (expressed as a percentage) between LF and LF+HF

3 EVALUATION AND RESULTS

The objective of the evaluation of the HR measurement method and the HRV parameters calculation method is primarily to optimize the different parameters (gain, sampling rate, ratios of the dynamic threshold, extrapolation of the fast periodogram, etc.) to ensure that the device will provide both the mandatory robustness and accuracy of the signals (and thus derived data) for the use of the sensor in clinical experiments and applications. On the other hand, it is necessary to maintain a suitable autonomy for long-term experiments by reducing power consumption of the overall device. In the proposed implementation, where the consumption of HR measurement method is already highly optimized by the use of dedicated hardware functions, further reduction of power consumption relies on the optimization of the calculation time of HRV parameters.

For this purpose, the REC Heart Activity sensor was evaluated both on a workbench in laboratory conditions as well as on individuals in real-life conditions as described in the next sections.

3.1 Accuracy of HR Assessment

Accuracy of the detection of R-peaks and the measurement of RR-intervals upon the ECG signal was evaluated using a hardware generated ECG. The Agilent 33220A is function / arbitrary waveform generator which provides a cardiac waveform. The amplitude, common-mode and frequency can be varied to verify the proper operation of the device in various conditions as those three parameters depends highly on the environmental and physical conditions of the individual (resting, effort), and also varies with the change of the electrode/skin interface over time (particularly when using dry electrodes).

The error in RR-intervals measurement was calculated as the mean difference between the period set on the generator and the period measured by the sensor. As the latter uses a counter with a frequency of 1024 Hz, the precision of RR-intervals measured is 0.98 ms. A dataset of 1000 RR-intervals was collected where intervals' length was linearly varied on

the generator from 400 ms (150 BPM) to 1200 ms (50 BPM), which is representative of most common heart rates. The mean value of all difference was -0.105 ms and the standard deviation of the differences was of 1.027 ms over all the range of RR-intervals. This difference corresponds to an error of 0.1 BPM when HR is 60 BPM, and 0.4 BPM when HR is 120 BPM which is lower than the usual 1 BPM resolution in standard devices.

3.2 Accuracy of PSD Estimation

To simulate heart rate variability and to evaluate the accuracy of the different implementation of the Lomb-Scargle periodogram, a known frequency modulation was applied to the ECG signal generated by the Agilent 33220A. The base HR was set at $f_{\text{base}} = 1.25$ Hz (75 BPM). The modulating signal was a triangular shape, with a frequency f_{mod} of 0.05 Hz and an amplitude of frequency deviation f_{dev} of 0.2 Hz. As the PSD is computed over RR-intervals in units of time (ms), the theoretical continuous function $RR(t)$ corresponding to the tachogram is given by Equations 6 and 7. The time variations of this continuous and periodic signal as well as the normalized PSD are shown on Figure 4.

$$x_{\text{tri}}(t) = 2 \left| 2 \left(t * f_{\text{mod}} - \left[t * f_{\text{mod}} + \frac{1}{2} \right] \right) \right| - 1 \quad (6)$$

$$RR(t) = \frac{1}{f_{\text{base}} + f_{\text{dev}} * x_{\text{tri}}(t)} \quad (7)$$

As shown on the normalized PSD, the use of a triangular shape as a modulating signal for HR has the advantage of inducing predictable harmonics in the PSD at multiple frequencies of the fundamental f_{mod} all over the range of interest 0.015-0.4 Hz. Additionally, the inverting relationship between RR-interval values and HR breaks the vertical symmetry of the triangular signal and thus adds even harmonics to the odd harmonics of the original triangular shape.

It therefore possible to analyse directly PSD obtains with different methods in order to compare both quality of PSD estimation and time of calculation. For this evaluation, the original Lomb-Scargle

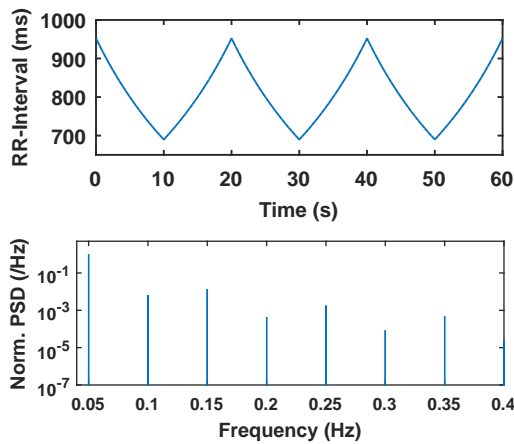


Figure 4: Theoretical continuous tachogram of generated RR-intervals and corresponding normalized PSD.

periodogram was implemented and optimized using trigonometric recurrences (Press, 2007). The fast implementation of the periodogram (Press and Rybicki, 1989) was also implemented, and tested with three different values for the MACC factor (1, 2 and 4).

Figure 5 shows the result of the different methods applied on RR-intervals during 5 minutes. Also Table 3 presents the calculation time for each method with the MCU set at its lower frequency (3 MHz) for reducing current consumption.

Table 3: Calculation time for each method of PSD estimation of RR-intervals for 5-minute long segments.

Type	Time (s)
Original LP	> 60
Fast LP (MACC = 4)	4
Fast LP (MACC = 2)	2.5
Fast LP (MACC = 1)	1

This results clearly shows that the original Lomb-Scargle implementation is not usable due to the especially long time of calculation (over 1 minute). However, the fastest implementation (MACC = 1) which takes only 1 second to calculate, adds considerable noise to the original PSD with a level around -70 dB. Finally the fast implementation with a MACC factor of 2 seems to be the best compromise between calculation time and noise level as it does not excess the level of the original one at -100 dB.

3.3 Evaluation of Power Consumption

Together with robustness and accuracy, one of the main objectives of the implementation of mixed hardware and software method for HR and HRV measurement is the optimization of power consumption of the

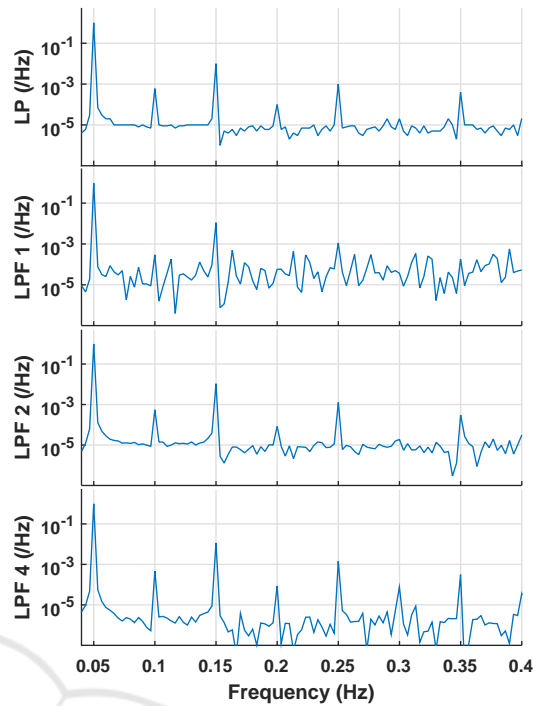


Figure 5: Normalized periodogram over of a generated 300-second buffer of RR-intervals using original Lomb-Scargle periodogram (LP) and its fast implementation for a MACC factor of 1,2 and 4 (LPF 1, LPF 2 and LPF 4 respectively).

REC Heart Activity Sensor. In this section we present and discuss the result of power consumption of the different parts of the system, composed of the analog ECG processing, analog to digital conversion of the signal, digital HR measurement, and software HRV calculation. Also additional power consumption due to wireless communication must be taken into account to estimate the overall consumption of the system.

Table 4 summarizes the power consumption of the different modules with the configuration used, by taking into account the duty cycle of module active time over a period of 5 minutes. The consumption of the RF module corresponds to a BLE connection with an Android device where every new HR and HRV values are sent in real time. The system is powered at 3.3 V using a linear voltage regulator having a negligible quiescent current and a 300 mAh one-cell Lithium-Ion battery, which enables to estimate the global autonomy of the sensor device.

The total resulting current consumption leads to a theoretical autonomy of 54 hours. This results is already large enough for very long term monitoring of cardiac activity during in-situ experiment. Indeed charging the battery, thanks to embedded micro-USB connector on the device, only less than 1 hour by using an ordinary USB charger. This can be done once

Table 4: Average current consumption of the different part of the REC Heart Activity sensor.

Module	Average current
Device base	1.83 mA
Radio module	0.82 mA
Analog Front-end	2.44 mA
Analog to digital conversion	0.25 mA
Hardware HR measurement	0.14 mA
Software HRV calculation	0.02 mA
Total	5.5 mA

every two days during a short period when the device is not used (for example it can be done during the daily time spent in the bathroom, where the device has to be removed).

On the other hand, the results show that a important contribution to the actual current consumption is due to analog front end which is composed of the integrated amplifiers for the differential amplification as well as the RLD circuit. This could be reduced by using existing discrete components which are optimized for low-power applications and then extends further the autonomy of the device with equal signal quality.

In conclusion, regarding the hardware HR measurement and HRV calculation methods, the evaluation has validated the advantage of combining available PLDs for real-time detection and measurement of HR with an optimized method for the calculation of short term HRV parameters, both in time and frequency domains, directly on the embedded system.

4 CONCLUSION

The objective of this study was to evaluate possibilities of taking advantage of a programmable system-on-chip in order to combine optimized methods for a complete, real-time monitoring and analysis of cardiac activity directly on a wearable sensor. This was done by using a PSoC5 LP, which combines :

- Integrated, programmable analog components, which were used to build the analog ECG front-end;
- Integrated digital filter components for a hardware R-peak detection and RR-interval measurement;
- 32-bit ARM Cortex M3 micro-controller unit for an embedded calculation of time-domain and frequency-domain HRV parameters.

The main advantage of using a PSoC5 LP was to have the entire ECG process, HR and HRV calculations fully integrated in a small, single chip. The Pan

and Tompkins' method for R-peak detection was implemented as a non-linear filter to benefits from the ultra-low power digital filter block, combined with a local maximum detector using a dynamic threshold for robust detection. The Press and Rybicki's fast algorithm for spectral analysis was adapted to provide a better estimation of PSD by the use of method dedicated to unvenly sampled data rather than FFTs, with fast enough calculation time compared to the original implementation of the Lomb-Scargle periodogram. A future optimization could be the use of a dedicated analog front-end rather than the integrated programmable-gain amplifiers which get higher current consumption than commercially available discrete components or ECG amplifiers.

However the REC Heart Activity sensor is already proposed as solution for a better real-time assessment of cardiac activity by providing not only HR measurement but also both time-domain and frequency-domain HRV parameters, calculated according to international standards for HRV analysis.

Moreover this device can be used within a wireless body sensor network, together with the sensors designed in the frame of the RECAMED project, as well as a software platform on smartphone for collecting, storing, and passing on data securely. This WBSN is proposed as a solution for the increasing clinical need of automated collection of health data from multiple patients, both inside and outside of a medical environment (hospital or nursing home).

ACKNOWLEDGEMENTS

The REC Heart Activity sensor is developed in the frame of the RECAMED project, funded by the BQR's program at INSA Lyon.

REFERENCES

- Altini, M., Polito, S., Penders, J., Kim, H., Van Helleputte, N., Kim, S., and Yazicioglu, F. (2011). An eeg patch combining a customized ultra-low-power eeg soc with bluetooth low energy for long term ambulatory monitoring. In *Proceedings of the 2nd Conference on Wireless Health*, page 15. ACM.
- Chen, Y.-H., Op de Beeck, M., Vanderheyden, L., Mihajlovic, V., Grundlehner, B., and Van Hoof, C. (2013). Comb-shaped polymer-based dry electrodes for eeg/ecg measurements with high user comfort. In *Engineering in Medicine and Biology Society (EMBC), 2013 35th Annual International Conference of the IEEE*, pages 551–554. IEEE.

- Clifford, G. D. and Tarassenko, L. (2005). Quantifying errors in spectral estimates of hrv due to beat replacement and resampling. *Biomedical Engineering, IEEE Transactions on*, 52(4):630–638.
- Go, A. S., Mozaffarian, D., Roger, V. L., Benjamin, E. J., Berry, J. D., Blaha, M. J., Dai, S., Ford, E. S., Fox, C. S., Franco, S., et al. (2014). Heart disease and stroke statistics—2014 update: a report from the american heart association. *Circulation*, 129(3):e28.
- Lomb, N. R. (1976). Least-squares frequency analysis of unequally spaced data. *Astrophysics and space science*, 39(2):447–462.
- Malik, M., Bigger, J. T., Camm, A. J., Kleiger, R. E., Malliani, A., Moss, A. J., and Schwartz, P. J. (1996). Heart rate variability standards of measurement, physiological interpretation, and clinical use. *European heart journal*, 17(3):354–381.
- Massot, B., Noury, N., Gehin, C., and McAdams, E. (2013). On designing an ubiquitous sensor network for health monitoring. In *2013 IEEE 15th International Conference on e-Health Networking, Applications and Services (Healthcom) (IEEE Healthcom 2013)*, Lisbon, Portugal.
- McAdams, E., Krupaviciute, A., Gehin, C., Grenier, E., Massot, B., Dittmar, A., Rubel, P., and Fayn, J. (2011). Wearable sensor systems: The challenges. In *Engineering in Medicine and Biology Society, EMBC, 2011 Annual International Conference of the IEEE*, pages 3648–3651.
- Pan, J. and Tompkins, W. (1985). A real-time qrs detection algorithm. *IEEE transactions on bio-medical engineering*, 32(3):230–236.
- Press, W. H. (2007). *Numerical recipes 3rd edition: The art of scientific computing*. Cambridge university press.
- Press, W. H. and Rybicki, G. B. (1989). Fast algorithm for spectral analysis of unevenly sampled data. *The Astrophysical Journal*, 338:277–280.
- Romero, I., Grundlehner, B., and Penders, J. (2009). Robust beat detector for ambulatory cardiac monitoring. In *Engineering in Medicine and Biology Society, 2009. EMBC 2009. Annual International Conference of the IEEE*, pages 950–953. IEEE.
- Scargle, J. D. (1982). Studies in astronomical time series analysis. ii-statistical aspects of spectral analysis of unevenly spaced data. *The Astrophysical Journal*, 263:835–853.
- Schäfer, A. and Vagedes, J. (2013). How accurate is pulse rate variability as an estimate of heart rate variability?: A review on studies comparing photoplethysmographic technology with an electrocardiogram. *International journal of cardiology*, 166(1):15–29.
- Shin, K., Minamitani, H., Onishi, S., Yamazaki, H., and Lee, M. (1994). The direct power spectral estimation of unevenly sampled cardiac event series. In *Engineering in Medicine and Biology Society, 1994. Engineering Advances: New Opportunities for Biomedical Engineers. Proceedings of the 16th Annual International Conference of the IEEE*, pages 1254–1255. IEEE.
- Van Hoof, C. and Penders, J. (2013). Addressing the health-care cost dilemma by managing health instead of managing illness: an opportunity for wearable wireless sensors. In *Proceedings of the Conference on Design, Automation and Test in Europe*, pages 1537–1539. EDA Consortium.
- Winter, B. B. and Webster, J. G. (1983). Driven-right-leg circuit design. *Biomedical Engineering, IEEE Transactions on*, 30(1):62–66.